catalysts

MDPI

Article

Experimental Study of CO_2 Conversion into Methanol by Synthesized Photocatalyst ($ZnFe_2O_4/TiO_2$) Using Visible Light as an Energy Source

Numair Manzoor [1], Muhammad Sadiq [2], Muhammad Naqvi [3,*], Umair Sikandar [4] and Salman Raza Naqvi [4]

[1] Engineer Distribution, Department of Health, Safety and Environment, Sui Northern Gas Pipelines Limited (SNGPL), Islamabad 46000, Pakistan; numair.manzoor@sngpl.com.pk

[2] The Joint Graduate School of Energy and Environment, King Mongkut's University of Technology Thonburi, KMUTT, Bangkok 10140, Thailand; mmsadiq@ksu.edu.sa

[3] Department of Engineering and Chemical Sciences, Karlstad University, 65188 Karlstad, Sweden

[4] School of Chemical and Materials Engineering, National University of Sciences and Technology, Islamabad 44000, Pakistan; umair.sikandar@scme.nust.edu.pk (U.S.); salman.raza@scme.nust.edu.pk (S.R.N.)

* Correspondence: raza.naqvi@kau.se

Received: 12 December 2019; Accepted: 14 January 2020; Published: 1 February 2020; Retracted: 16 March 2022

check for updates

Abstract: Ozone layer depletion is a serious threat due to the extensive release of greenhouse gases. The emission of carbon dioxide (CO_2) from fossil fuel combustion is a major reason for global warming. Energy demands and climate change are coupled with each other. $CO_2$is a major gas contributing to global warming; hence, the conversion of CO_2 into useful products such as methanol, formic acid, formaldehyde, etc., under visible light is an attractive topic. Challenges associated with the current research include synthesizing a photocatalyst that is driven by visible light with a narrow band gap range between 2.5 and 3.0 eV, the separation of a mixed end product, and the two to three times faster recombination rate of an electron–hole pair compared with separation over yield. The purpose of the current research is to convert CO_2 into useful fuel i.e., methanol; the current study focuses on the photocatalytic reduction of CO_2into a useful product. This research is based on the profound analysis of published work, which allows the selection of appropriate methods and material for this research. In this study, zinc ferrite ($ZnFe_2O_4$) is synthesized via the modified sol–gel method and coupled with titanium dioxide (TiO_2). Thereafter, the catalyst is characterized by Fourier transform infrared (FTIR), FE-SEM, UV–Vis, and XRD characterization techniques. UV–Vis illustrates that the synthesized catalyst has a low band gap and utilizes a major portion of visible light irradiation. The XRD pattern was confirmed by the formation of the desired catalyst. FE-SEM illustrated that the size of the catalyst ranges from 50 to 500 nm and BET analysis determined the surface area, which was 2.213 and 6.453 m^2/g for $ZnFe_2O_4$ and $ZnFe_2O_4/TiO_2$, respectively. The continuous gas flow photoreactor was used to study the activity of the synthesized catalyst, while titanium dioxide (TiO_2) has been coupled with zinc ferrite ($ZnFe_2O_4$) under visible light in order to obtain the maximum yield of methanol as a single product and simultaneously avoid the conversion of CO_2 into multiple products. The performance of $ZnFe_2O_4/TiO_2$was mainly assessed through methanol yield with a variable amount of TiO_2 over $ZnFe_2O_4$ (1:1, 1:2, 2:1, 1:3, and 3:1). The synthesized catalyst recycling ability has been tested up to five cycles. Finally, we concluded that the optimum conditions for maximum yield were found to be a calcination temperature of $ZnFe_2O_4$at 900 °C, and optimum yield was at a 1:1 *w*/*w* coupling ratio of $ZnFe_2O_4/TiO_2$. It was observed that due to the enhancement in the electron–hole pair lifetime, the methanol yield at 141.22 $\mu mol/g_{cat}\cdot h$ over $ZnFe_2O_4/TiO_2$was found to be 7% higher than the earlier reported data.

Keywords: methanol; CO_2 reduction; $ZnFe_2O_4/TiO_2$; photocatalyst; band gap energy

This paper has been retracted.
A retraction notice was published on 16 March 2022 in *Catalysts* **2022**, *12*, 336; doi:10.3390/catal12030336

1. Introduction

Depletion of the ozone layer is not only a serious threat due to the extensive release of greenhouse gases; the emission of $CO_2$is also a major reason for global warming. Current global demand for energy is almost 17 TW (Terawatt) and is forecasted to be doubled in upcoming years [1]. The climate change committee i.e., the IGP (Intergovernmental Panel), recommends that emissions of CO_2 must be reduced by up to half of the total 85% reduction target by 2050 [2]. Reports of the Kyoto Protocol revealed that the countries under the Kyoto Protocol produce 22.5% less CO_2 compared to production back in 1990. The carbon capture and storage techniques (CCS) are highly uneconomical for medium and small plants, and that is a major drawback [3].

For the effective conversion of CO_2 into useful products such as methane, methanol, formic acid, etc., many researchers/scientists suggested different techniques from electrochemical cell to thermal decomposition. Thus, electrochemical cells have a superior advantage over thermal decomposition due to sustainable energy utilization i.e., visible light/sunlight, etc.

There are several processes where CO_2 can be converted into market useful products; CO_2 can be captured by using following techniques: (a) before the combustion capturing of CO_2, (b) in-process capturing by adjusting the oxygen–fuel ratio, and (c) after combustion capturing of CO_2. Considering all of the said techniques, the most researched and discussed option is post combustion CO_2 capturing and conversion. Many catalytic/photocatalytic materials have been utilized for the conversion of CO_2into useful products i.e., TiO_2/SB (SB/Antimony) used for the conversion of carbon dioxide into CH_3OH, Ag Br/CNT (CNT, or carbon nanotubes) used for the conversion of carbon dioxide into CH_3OH and C_2H_5OH, CdSe/Pt/TiO_2 used for CH_4, CH_3OH, etc. Factors such as photo corrosion resistance, valance and conduction band positions, accessibility, cost, surface area, ease of availability, etc. are the most important factors in the selection of photocatalysts, in which our selected photocatalyst i.e.,$ZnFe_2O_4/TiO_2$ is ahead of the other visible light-induced photocatalysts. The most viable catalyst is $ZnFe_2O_4/TiO_2$ in terms of valance and conduction band position, resistance toward corrosion, cheap cost, and stability; all of these above-mentioned factors make this photocatalyst most suitable for conversion within a visible range and maximum yield of the specific product i.e., methanol.

Different products can be obtained through the reduction of CO_2, as shown in Table 1. Despite the market demanding products from the CO_2 reduction reactions, still much work needs to be done in this field.

Table 1. CO_2 reduction and market sales potential of different products formed by CO_2 conversion.

Product	Potential of CO_2Reduction (ton CO_2/ton of Product)	Market Scale (per Year)		References
		Global Demand (million ton, MT)	Market Value (billion $)	
Dimethyl ether (DME)	1.9	6.3	3.2	[4]
Dimethyl carbonate (DMC)	1.47	0.24	280	—
Polycarbonate	0.5	3.6	14.4	[4]
Methanol	1.38	75	36	[5]
Urea	0.735-0.75	198.4	59.5	[6]

The utilization of value-added products from CO_2conversion such as methanol seems to be a most promising technique to reduce the effect of major greenhouse gases (CO_2) on the atmosphere. The photocatalytic reduction of CO_2 depends upon the hydrogen produced during water splitting, because water is the most common reductant used for this reaction. During the reduction reaction, more than one product obtained formaldehyde or formic acid. The photocatalytic splitting of water is a simple process because only two products are obtained by this reaction: hydrogen and oxygen. On the other hand, the photocatalytic reduction of CO_2 is a complex reaction because more than one product is obtained during the reaction, and still, no full complete explanation for the product selectivity is available. Researchers found that during the reduction of CO_2, the first product that was formed was formic acid, which converts into formaldehyde, and the formaldehyde finally converts into methanol. However, on the other hand, some studies indicated that product selectivity can be controlled by the position of the conduction band of the photocatalyst. Other products can also be produced during the reaction such as formaldehyde, hydrogen, ethanol, and CO, but they are not detected in this study.

The purpose of the current research is to convert CO_2 into useful fuel i.e., methanol. For this objective to be achieved, we first synthesize the $ZnFe_2O_4/TiO_2$ photocatalyst, and afterwards characterize a $ZnFe_2O_4/TiO_2$heterojunction photocatalyst to check whether our desired specified catalyst has been synthesized or not. Then, we evaluate the activity of the prepared photocatalyst for CO_2conversion into methanol under visible light (initially, a tungsten bulb is used, but we aim to get conversion through sunlight/renewable energy). Starting from the energy of +805 kJ/mol is required for the bond breakage of chemically stable CO_2 due to its carbon–oxygen bonds. A carbon-free energy source such as solar light can be used for this purpose under the presence of a photocatalyst. The photocatalysis process continues only if there is suitable photon energy of light UV/visible light. Research works in the literature reported that the obtained yield and selectivity of the product was very low in CO_2 photocatalysis under visible light [7]. The conversion of carbon into useful fuel required a sustainable amount of hydrogen i.e., some suitable source of hydrogen such as H_2 and H_2O, etc. The cheapest and most easily available source is water. During the photocatalysis of $CO_2$with water, water splitting also competes with CO_2 reduction reaction because water splitting is much simpler than CO_2reduction. This is because the splitting of water into H_2 and O_2 is a two-electron process, but CO_2conversion into methanol required six electrons and six protons [8]. Moreover, the position of the conduction band plays an important role for CO_2 conversion into the desired product. Different types of photocatalysts were prepared and tested by various research groups in the last few decades for the conversion of CO_2into methanol such as metal oxides, layered double hydroxides and metal ferrite [9,10]. $ZnFe_2O_4$ works under visible light due to its smaller band gap and transferred electrons to TiO_2 because it is a p-type semiconductor and TiO_2 is n-type based; based on the previous study, that the $ZnFe_2O_4$ coupled with TiO_2 can be synthesized as an efficient visible light drove the photocatalyst for CO_2 reduction. However, TiO_2 is identified as one of the best photocatalysts due to its cost and stability [3]. The major problem in TiO_2 is its large band gap of approximately 3.2 eV [11]. The large band gap of TiO_2 makes it a UV–Vis-driven photocatalyst.

In order to obtain the high selectivity of a given product and the maximum yield of the desired product, water and CO_2 used as raw feed, oxidation also has the same importance as CO_2. Both components are stable, and their bond breakage is possible by using a carbon-free sustainable source of energy as a solar light in the presence of a photocatalyst. The maximum Faradaic efficiency of hydrocarbons was observed at −1.9 V with 40.3%; similarly, hydrogen formation could be depressed to 34.7%. During the reduction of CO_2 with water, the most favorable reaction is water reduction instead of CO_2 due to this huge difference in their reduction potential. This problem of water reduction instead of CO_2 can be solved by the oxidation of water instead of reduction. For water oxidation, the photocatalyst must have a valence band edge that is more positive than water oxidation, which is +0.82 eV. The most common reaction that happened during the reduction of CO_2 with water at 7pH is tabulated below in Table 2.

Table 2. Thermodynamic potential of CO_2 into different products.

Sr. No.	Reaction	Thermodynamic Potential V vs. NHE (Normal Hydrogen Electrode)	
		V vs. NHE	Reference
1	$CO_2 + e^- \rightarrow CO_2^-$	−1.9	[3]
2	$CO_2 + 2H^+ \rightarrow HCOOH$	−0.61	[11]
3	$2H^+ + e^- \rightarrow H_2$	−0.41	[3]

The most common problem associated with photocatalysis by these catalysts is the conversion of CO_2 to more than one product [12]. Thus the reaction mechanism, the effect of the amount of catalyst loading, the influence of calcination temperature, and the effect of the recycled catalyst during photoactivity are investigated thoroughly.

2. Results

2.1. Characterization

The following characterization techniques have been used on order to confirm the exact formation of the desired photocatalyst, but these techniques have been limited to some extent, as our main focus is to study the experimental effects of the different parameters.

2.1.1. FTIR (Fourier Transform Infrared Spectroscopy)

A Shimadzu spectrometer in the range of 4000–450 cm^{-1}used for recording the FTIR spectra. The catalyst was in powdered form, and the formation of $ZnFe_2O_4$ was confirmed by using FTIR data as a preliminary result. The FTIR spectra recorded using a spectrometer in the range of 4000–450 cm^{-1}, which is comparable to previously reported results [13]. The catalyst was in powdered form, and the formation of $ZnFe_2O_4$ was confirmed i.e., the spectrum band at 592.5 cm^{-1} and 487.3 cm^{-1} represents Zn^{2+} and Fe^{3+} ions, as shown in Figure 1. Moreover, the FTIR spectrum of $ZnFe_2O_4$ - TiO_2 exhibits peaks having main characteristics of TiO_2 at 487.3 cm^{-1} and $ZnFe_2O_4$ at 592.5 cm^{-1}. In the same way, the band at 1488.6 cm^{-1} points toward the sample containing a slight amount of water. The band at 1253.1 cm^{-1} is an indication of the presence of nitrates. The presence of water is mainly due to the modified method of synthesis; nitrates were present because the synthesis starts from the nitrates of metals. The last peaks at 2401.7 cm^{-1} and 3248.8 cm^{-1} indicate the presence of CO_2 that was absorbed into the catalyst synthesized from the environment. Some peaks can be witnessed, which are major and show good agreement with those of $ZnFe_2O_4$–TiO_2 nanocomposites, ensuring that the presence of functional groups on the surface of $ZnFe_2O_4$–TiO_2 are due to octane residues, as evident in Figure 1.

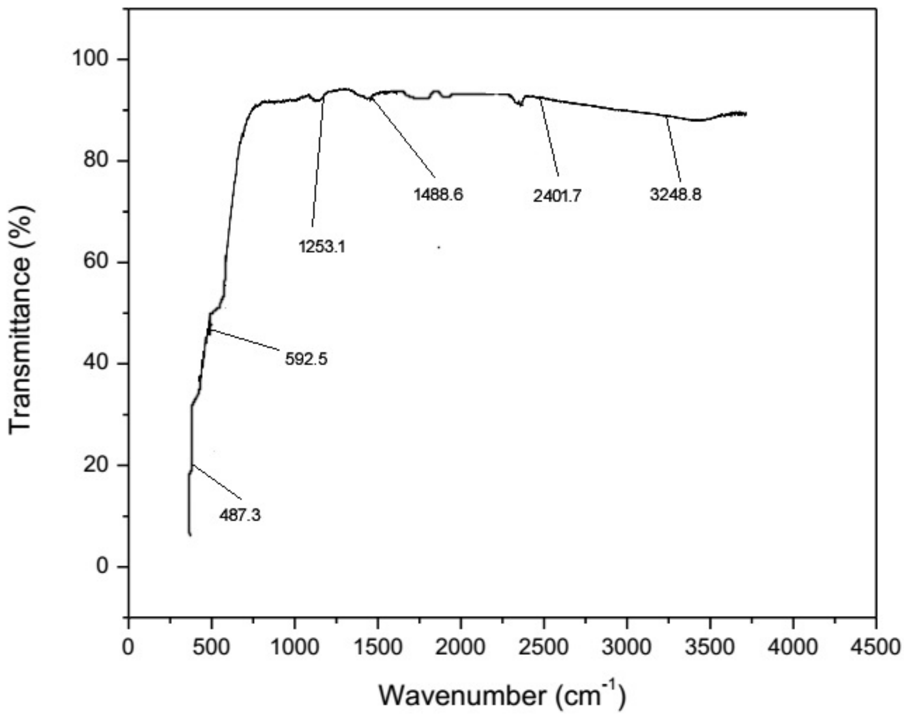

Figure 1. Fourier transform infrared (FTIR) analysis of the $ZnFe_2O_4/TiO_2$photocatalyst performed on 4000–450 cm^{-1}range spectrophotometer.

2.1.2. UV–Vis Spectroscopy

The UV–Vis spectroscopy of synthesized catalysts $ZnFe_2O_4/TiO_2$, $ZnFe_2O_4$, and TiO_2 was done at a wavelength range of 200–800 nm. This absorption spectrum of the catalyst revealed that the synthesized catalyst is the product of visible light active range of the catalyst. A wavelength of 200–800 nm has been used for studying the UV–Vis spectroscopy of the synthesized catalysts $ZnFe_2O_4/TiO_2$(1:1), $ZnFe_2O_4$, and TiO_2. The absorption spectrum of the synthesized catalyst revealed that it is a visible light active photocatalyst; the UV–Vis spectra of synthesized $ZnFe_2O_4$, TiO_2, and $ZnFe_2O_4$ coupled with TiO_2 in different *w*/*w* ratios in the wavelength range of 200–800 nm is shown in Figure 2. $ZnFe_2O_4$ shows a good absorbance pattern from 400–800 nm, which reveals that it is an excellent photocatalyst [14]. TiO_2 illustrates absorbance only from 200 to 400 nm, which concludes that it is a UV active photocatalyst. When $ZnFe_2O_4$ is coupled with TiO_2 in a 1:1 weight/weight ratio, it clarifies visible light region maximum absorbance from 400 to 800 nm. The absorbance pattern of the remaining two ratios is also illustrated in Figure 2. Moreover, another two ratios also display absorbance under visible light region, but the absorbance is comparatively lower than a 1:1 ratio. These three ratios show transparency above 516 nm, 442 nm, and 427 nm, which indicates that all three ratios have shifted the band gap of commercialized TiO_2 from an ultraviolet region to visible light. The most suitable ratio that covers the majority of the visible light region is 1:1. The coupling of a low band gap $ZnFe_2O_4$ with TiO_2 reduces the band gap, and the proper ratio of both semiconductors is 1:1. This ratio efficiently minimizes the band gap of coupled semiconductors and absorbs a maximum portion of visible light. TiO_2 shows an absorbance pattern only under the UV region. After extrapolation, a line has been produced that shows the photon energy axis and produces the semiconductor band gap.

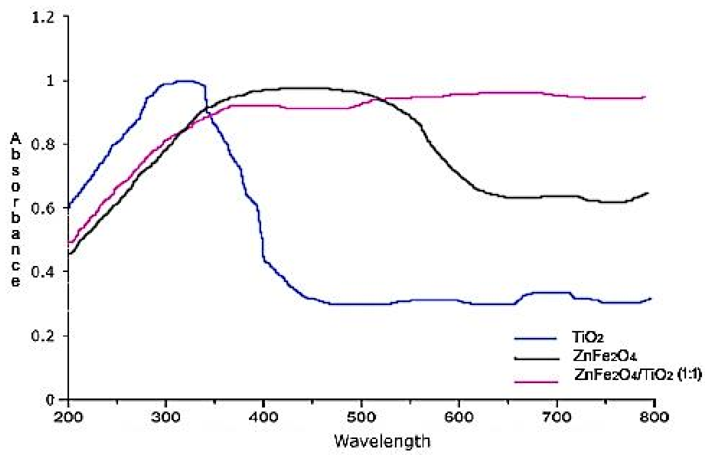

Figure 2. UV–Vis spectra of the synthesized photocatalyst; the wavelength set was 200–800 nm.

The band gaps of TiO_2, $ZnFe_2O_4$, and $ZnFe_2O_4$coupled with TiO_2 (1:1) are 3.15, 1.86, and 2.79 eV, respectively. $ZnFe_2O_4$ shows maximum absorbance at 624 nm and is well matched with previously reported results. The coupling of $ZnFe_2O_4$ with TiO_2 in a proper ratio shifts the band gap of TiO_2 from the UV region to the visible region and is used efficiently for the reduction of CO_2 into methanol under visible light irradiation.

2.1.3. FE-SEM Analysis

The possible accumulation and morphologies due to the tiny crystallites contact of synthesized catalysts were determined by using FE-SEM (field emission electron scanning electron microscope). This technique also pointed out the particle size of the synthesized catalyst. The magnification was done from 10 to 150. The following results shows that the $ZnFe_2O_4$:TiO_2 nanocomposites are regularly shaped nanoparticles. The $ZnFe_2O_4$ synthesized formed well-defined crystalline irregular spherical shapes with particle sizes in the range of 200–400 nm (Figure 3a,b). The anatase TiO_2 is also observed to be more homogeneous with high crystallinity. The particle size of TiO_2 nanoparticles is found to be in the range of 50–300 nm (Figure 3c,d). However, the $ZnFe_2O_4/TiO_2$was attributed to the magnetic property of $ZnFe^{I}{}_2O_4$ particles. It is observed that the $ZnFe_2O_4/TiO_2$ heterojunction with a (1:1) ratio shows high homogeneity and porosity (Figure 3e,f). It is observed that a hydrothermally developed $ZnFe_2O_4$:TiO_2 (1:1) heterojunction followed by annealing at 500 °C instigates higher homogeneity in the photocatalyst. The corresponding elements of the heterojunction such as Ti, O, Zn, and Fe show better homogeneity in the structure, while post annealing may promote the interfacial contact between $ZnFe_2O_4$ and TiO_2 nanostructures (Figure 3). Moreover, an interface/boundary is witnessed between two nanoparticles, indicating the presence of a heterojunction between $ZnFe_2O_4$ and TiO_2 which can further enable the charge transfer more freely to expressively reduce electron–hole pairs recombination in addition to enhancing the visible light-driven photocatalytic activity of $ZnFe_2O_4$:TiO_2 nanocomposites. It illustrates the importance of the development of a heterojunction by hydrothermal modification followed by post-sintering treatment.

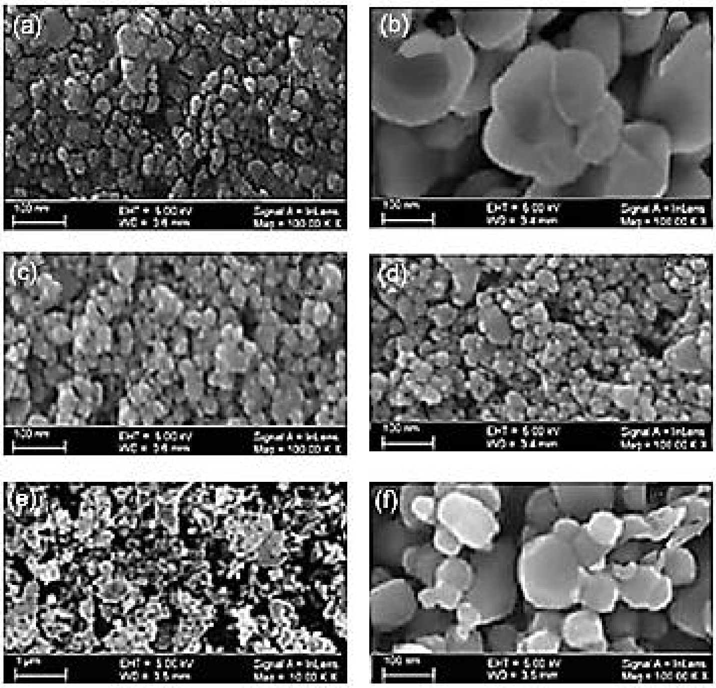

Figure 3. Images (**a**,**b**) $ZnFe_2O_4$, (**c**,**d**), and (**e**,**f**) $ZnFe_2O_4$:TiO_2 (1:1).

2.1.4. XRD Spectra

The synthesized catalyst is characterized by XRD for the identification of crystallinity. CuKα (1.542Å) radiation is used. The XRD scan range is 10–80°, the accelerating potential was 40 KVA, and the scan step size was 0.02°. The XRD pattern of $ZnFe^{I}{}_2O_4$, TiO_2, and $ZnFe_2O_4/TiO_2$ (1:1 *w*/*w* ratio) is shown in Figure 4. The XRD pattern of TiO_2 illustrates that it is available in anatase phase and all the peaks are well matched. $ZnFe^{I}{}_2O_4$peaks prove that it is in the spinel phase. No peak shift or extra peak are observed after coupling, which means that no impurity is induced into it after the coupling of both semiconductors, and the pure catalyst retained its previous phase. The crystalline sizes of $ZnFe_2O_4$, TiO_2, and $ZnFe_2O_4$:TiO_2 (1:1) are 44.8, 65.2, and 46.9 nm.

2.2. Conversion of CO_2 into Methanol Using Photocatalyst

Approximately 7 h has been taken in order to study the photocatalytic conversion of CO_2 into methanol by using $ZnFe_2O_4/TiO_2$ photocatalysts. The ratio used here is the one that gives the maximum yield of methanol, i.e., $ZnFe_2O_4/TiO_2$ (1:1 *w*/*w*); moreover, 7 h has been taken by considering previous research and literature [2,15]. The experimental results reveal that methanol is a major product in liquid, while the photoactivity of metal ferrite decreases, which is a clear indication of the exhaust of active sites due to photo corrosion. The other catalysts such as metal, non-metal, or S-S doped TiO_2 or other than TiO_2 also show the deactivation after 7 h. Hence, a 7 h irradiation time was chosen based on the previous work. In a current study, the catalyst has shown deactivation after 5.5 h. The highest yield is obtained after 5.5 h, which is 531.6 µmol/L·g_{cat}, but after that, the yield of methanol decreases, which is due to the conversion of CO_2 into other products or the occurrence of a backward reaction [16,17].

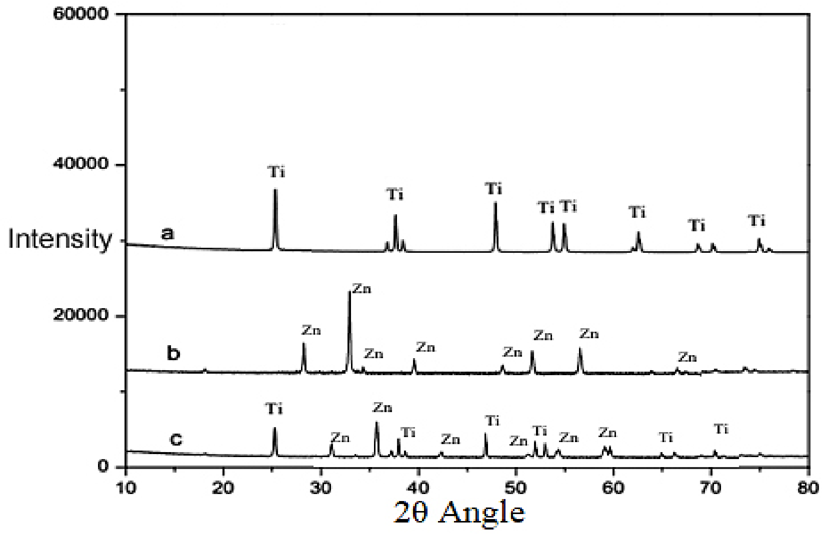

Figure 4. XRD spectra (**a**) TiO_2, (**b**) $ZnFe^{I}_2O_4$, and (**c**) $ZnFe^{I}_2O_4$:TiO_2 (1:1).

The Figure 5 indicates that the yield is increasing with a continuous passage of time, but after 5.5 h, the yield declines suddenly. Methanol oxidation occurred instead of water oxidation, which is one of the major reasons for yield diminution [17]. Similarly, as Figure 5 indicates, after of visible light irradiation, the photoactivity of metal ferrites reaches its high point, indicating that all the active sites are exhausted [18].

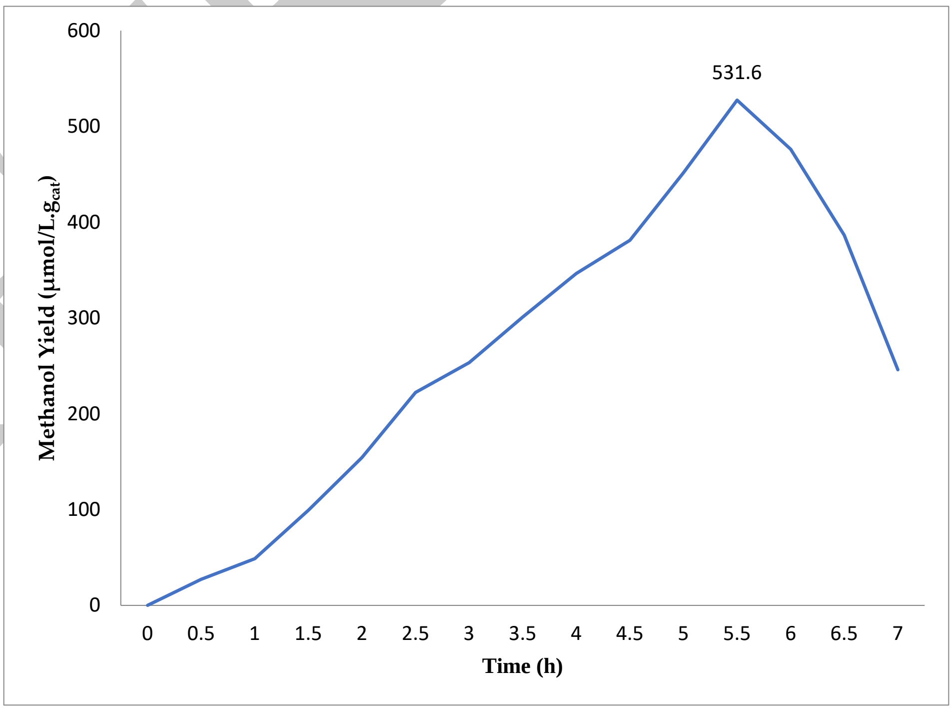

Figure 5. The activity of the$ZnFe_2O_4$/TiO_2 (1:1 *w*/*w*) photocatalyst.

2.3. Effect of Different Coupling Ratios of $ZnFe_2O_4$ with TiO_2

A different coupling ratio effect has been studied and finally plotted on the graph as shown in Figure 6, which reveals that $ZnFe_2O_4/TiO_2$ in a 1:1 *w*/*w* ratio produces a higher yield. This has also been evident from the FTIR analysis when 1:1 coupling shows maximum absorbance, too. Other coupling ratios have also been tested i.e., $ZnFe_2O_4$ is coupled with TiO_2 in a 1:2 ratio, while the yield of methanol is decreased upto 30% as compared to a 1:1 ratio. In the case of a 1:2 ratio, it can be suggested that the majority of the catalyst is TiO_2, which can work only under UV light such that only a small portion of$ZnFe_2O_4$is sensitized to TiO_2. This is the main reason behind the yield depression. Similarly, when $ZnFe_2O_4$ is coupled with TiO_2 in a 2:1 ratio, then the yield is much less. Correspondingly, the yield for the ratios of 1:3 and 3:1 has also been so minimal that it has also vanished. We can say the optimum methanol yield in comparison with the 1:1 ratio is 702.11µmol/g_{cat}, and the yield is decreased up to 30% by using a 1:2 ratio. Up to 70% less methanol is obtained when a 2:1 ratio is used. Moreover, the yield has drastically decreased i.e., by 86.9% and 87.3% for 1:3 and 3:1, respectively.

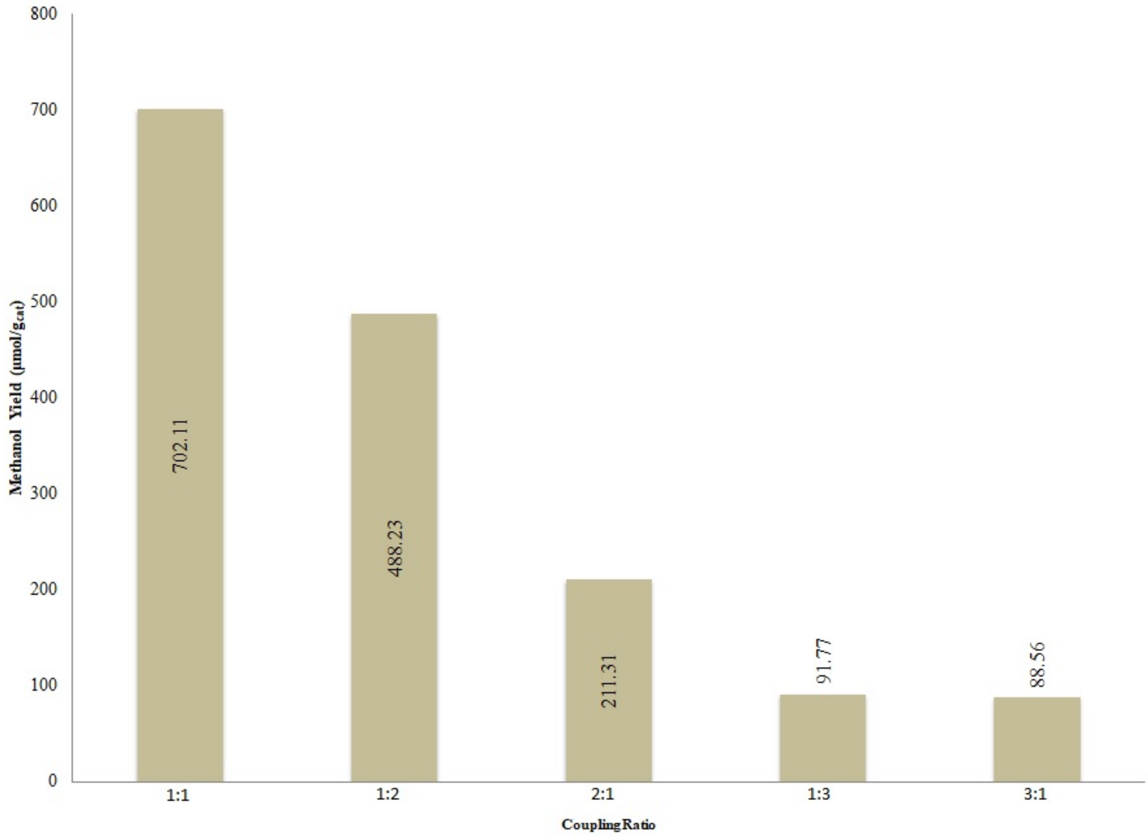

Figure 6. Effect of different coupling ratios on methanol yield.

2.4. Variable Calcination Temperature of $ZnFe_2O_4$ Effects

For synthesized photocatalysts calcined at different temperatures, the effect of different calcination temperatures on the methanol yield is illustrated in Figure 7. The catalyst was exposed under visible light irradiations for 5.5 h to check the photoactivity. The trend reveals that the amount of methanol is directly proportional to calcination temperature from 600 to 1000 °C. However, a sudden decrease in yield is observed when the calcination temperature is increased from 900 to 1000 °C. The increase in methanol yield with the increase in calcination temperature from 700 to 900 °C is due to the removal of all the impurities and volatile matters. The methanol yield obtained at 900 °C calcination temperature is 51% higher in comparison to a catalyst calcined at 700 °C and 36% greater than the catalyst calcined at 800 °C. Moreover, as the calcination temperature raise from 900to 1000 °C, an 85% decline in the yield is achieved in comparison with 900 °C calcination temperature. It is recommended that at >900 °C, the $ZnFe_2O_4$obtains impurities and the majority of active sites are deactivated, which results in a sudden dispersion in yield. As the temperature increases, the peak intensity increases and negligible peaks become clearer such that the crystallinity and shape of the crystals change [19,20].

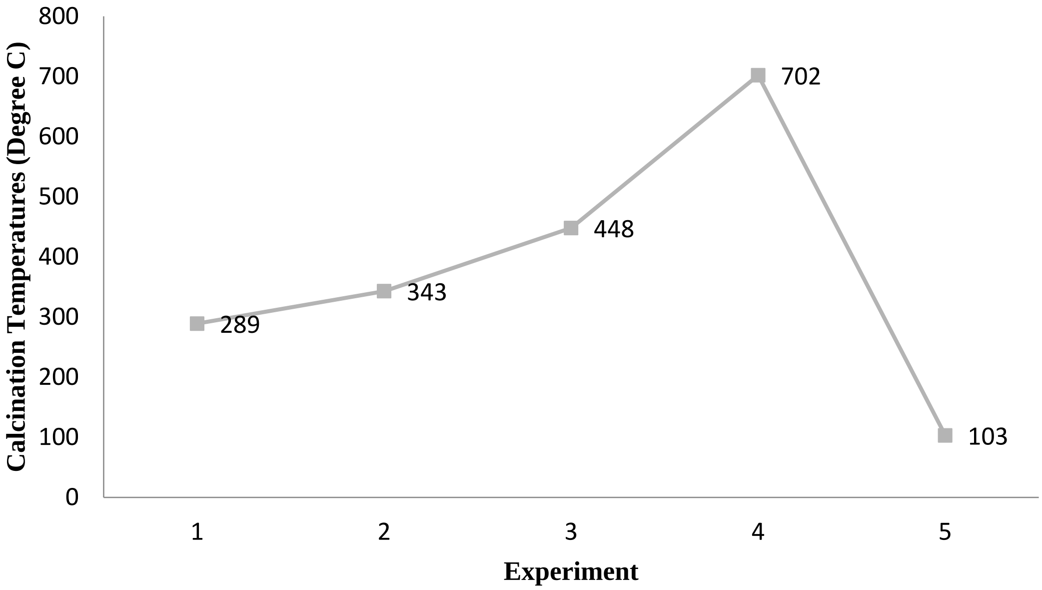

Figure 7. Effect of calcination temperature on yield.

2.5. Effect of Different Catalyst Loading Ratios

To understand the effect of catalyst loading on the reduction of CO_2 into methanol, different loading ratios were used ranging from 0.5 to 3 g/L, and the results are represented in Figure 8. It is apparent that the amount of methanol (μmol/L) increases as the amount of loaded catalyst increases from 0.5 to 3 gm/L.

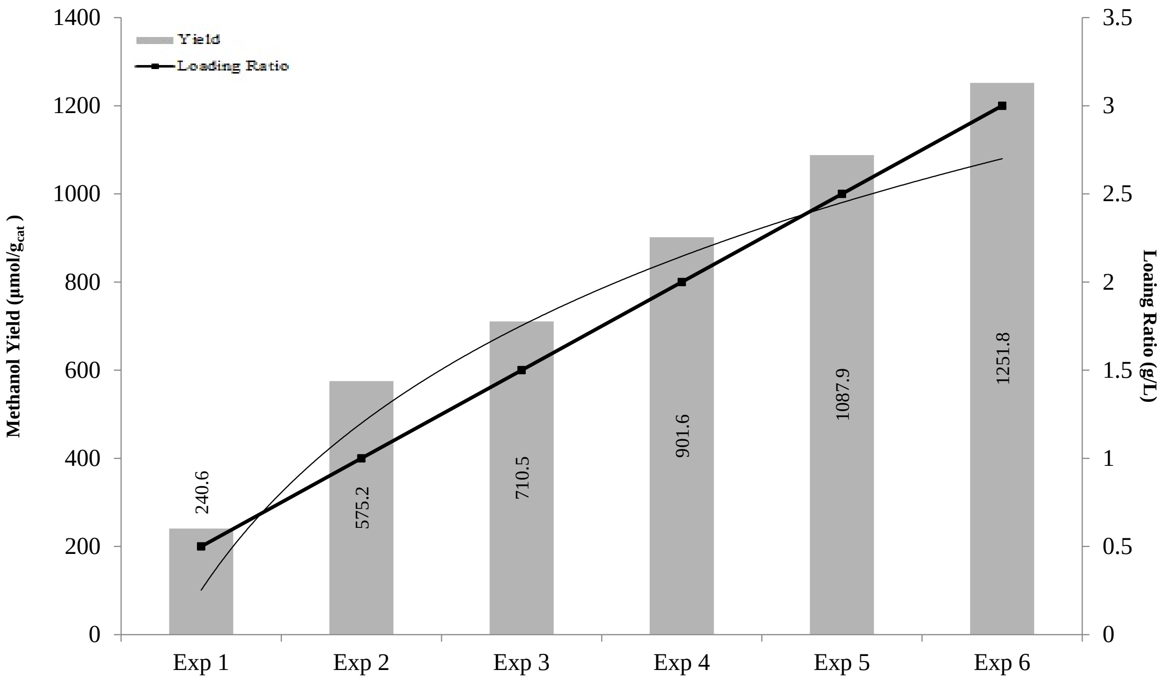

Figure 8. Effect of different catalyst loading ratios on the yield of methanol.

Table 3 will further clarify that at which loading ratio quantity, Methanol yield will be optimum etc.

Table 3. Methanol yield with respect to loading ratios.

Experiments	Loading Ratio (g/L)	Methanol Yield (µmol/g_{cat})
1	0.5	240.6
2	1	575.2
3	1.5	710.5
4	2	901.6
5	2.5	1087.9
6	3	1251.8

The trend in Figure 8 shows an incremental increase; however, it is not exactly proportional to the amount of the catalyst loading ratio. The yield of methanol is 240.60 µmol/g_{cat} by using 0.5 g/L catalyst. As the amount of catalyst is increased from 1 to 2 g/L, the amount of methanol should be doubled theoretically. However, only 36.2% higher methanol is obtained by using 2 g/L and vice versa. Moreover, the ratio percentage shows that the maximum yield is at 1 g/L, i.e., at 2 g/L, it must be double or near to that, but in the original, it is much lesser than that of 1 g/L, and the reverse is true until 3 g/L. Thus, at 1 g/L, the yield is 57.5%; at 2 g/L, the yield is 45.8%; and at 3 g/L, the yield is 41.7%. So, the optimum loading ratio is 1g/L, as the maximum yield has been obtained as per the loading ratio.

2.6. *Effect of Catalyst Recycling*

The catalyst has been recycled five times, and experimentation afterwards shows the trend of the recycling effect, as illustrated in Figure 9. After the first run, the whole solution present in a reactor including the catalyst was centrifuged at 1700 rpm for 18 min, and the catalyst was separated during the centrifuged process. The obtained catalyst was dried in an oven for 14 h at 120 °C. It is observed that activity of the catalyst decreases almost up to 55% during the second run. During the third run, a further decrease in the yield is observed, but this is not a straight-line depression in yield. For further standing, calculations of the trend of the decrease in the fourth and fifth run of the catalyst have also been done, which show that the yield has exponentially dropped by the fifth time run. It can be suggested that after 5.5 h, all the active sites are deactivated, and after recycling again and again, only a few sites are able to become active. It can be concluded that the catalyst is not useable again efficiently. Secondly, it is not possible to separate all the catalysts; however, the major portion is separated effectively. The deficiency of the catalyst is fulfilled by adding a fresh catalyst. The results clearly indicate that the catalyst can be effectively used only for one run. The metal ferrites do not work efficiently after recycling, because photo corrosion is a basic problem associated with this class [21,22].

Thus, it can be said that a similar trend has been observed in the current study. Methanol production via a CO_2 reduction mechanism through a $ZnFe_2O_4/TiO_2$ photocatalyst is illustrated in Figure 10.

It can be clearly understood from the yield experiment that after 5.5 h, the active sites become deactivated and after recycling, only just a few sites become active; thus, the main sites remain deactivated. Finally, it can be concluded that the catalyst is non-usable again and again effectively and efficiently. Thus, we can conclude from the said findings that the catalyst could only be used once efficiently. Moreover, the ferrites of metal did not work efficiently after recycling, the reason behind which could be the photo corrosion, etc.

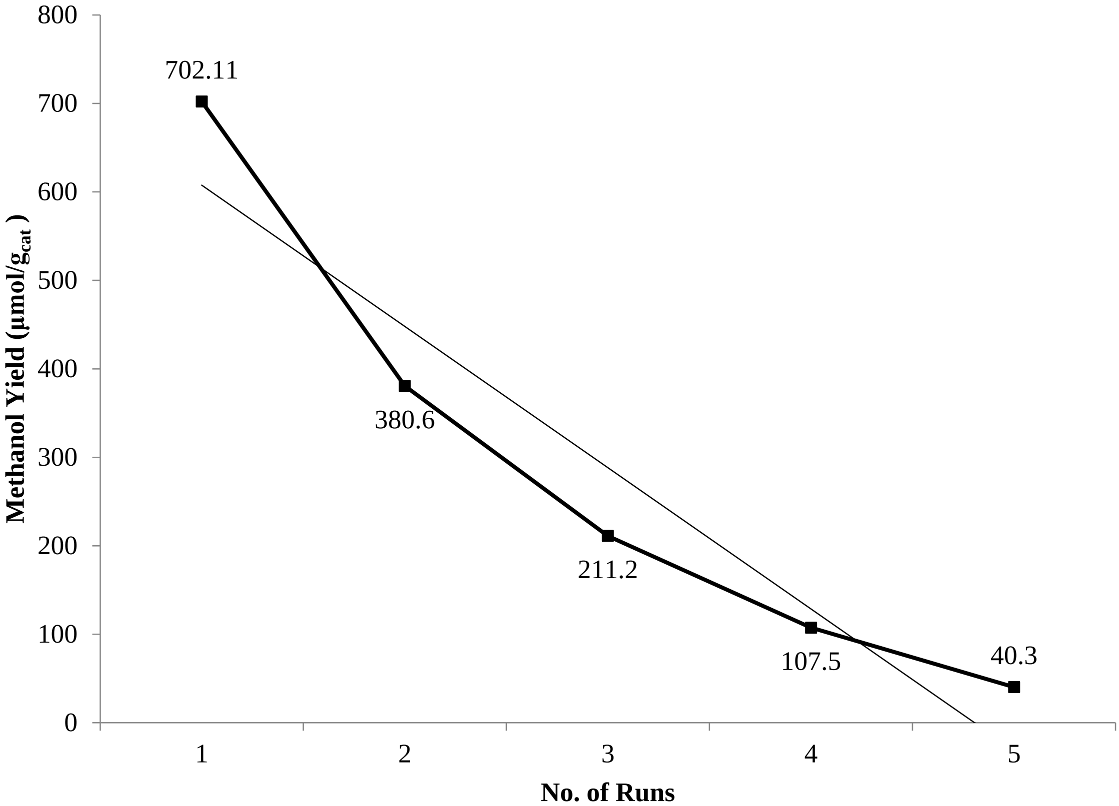

Figure 9. Effect of recycling a catalyst on the yield of methanol.

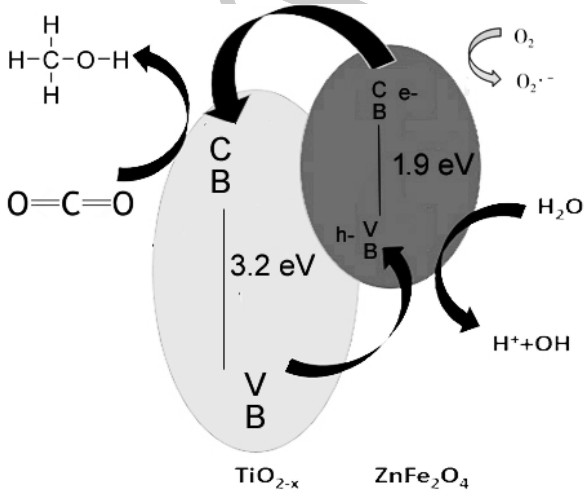

Figure 10. Proposed reaction mechanism.

2.7. Proposed Reaction Mechanism

In Figure 10, a reaction mechanism of the carbon conversion into methanol has been proposed, the pH was 6.2 during the experimentation such that CO_2 could not only exist as dissolved CO_2 but also in the form of HCO_3^-. The most abundant form of CO_2 at this pH is the dissolved CO_2 and HCO_3^-.

$$[H^+] = [OH^-] + [HCO_3^-] + [2CO_3^{2-}]$$

The coefficient 2 in above expression indicates that 2 moles of H^+ are required for the conversion of CO_3^{2-} into HCO_3^-, which is considered as a reference level. The pH during the reaction was maintained at 6.2, which is acidic, such that all the bicarbonates that can be produced in CO_2 and water mixture can be neglected.

The conversion of CO_2occurs on this surface of TiO_2 and water oxidizes on the surface of $ZnFe_2O_4$ because holes are transferred from TiO_2 to $ZnFe_2O_4$ due to the position of its valence band.

The CB (Conduction Band) position of $ZnFe_2O_4$ is more negative than the CB of TiO_2, and its position is also close to the reduction potential of CO_2 into methanol. So, under the presence of visible light irradiation, the excited electrons are transferred from the VB (Valance Band) of $ZnFe_2O_4$ to the CB of $ZnFe_2O_4$. These excited electrons are easily transferred to TiO_2 because of the formation of a heterojunction between these two semiconductors. Secondly, TiO_2 is also available in the Ti^{3+} state, which is more active than the Ti^{4+} state. Therefore, the efficiency also increases due to this reason. During the photoexcitation process, the holes are also generated that are transferred to the VB of $ZnFe_2O_4$, as illustrated in Figure 10. The heterostructure increases the e- and h+ separation time. Therefore, the recombination rate of e- and h+ is very slow, which is very suitable for photocatalytic reactions. The conversion of CO_2 occurs on this surface of TiO_2, and water oxidizes on the surface of $ZnFe_2O_4$ because holes are transferred from TiO_2 to $ZnFe_2O_4$ due to the position of its valence band. The yield of methanol is slightly higher than the recently reported results, which are 651μmol/g_{cat}. The increase in yield is suggested due to the proper alignment of $ZnFe_2O_4$ with TiO_2. Moreover, the constant temperature during the reaction and higher intensity of light are other reasons to get a higher yield.

2.8. Comparison with Previous Results

As TiO_2 cannot be used only for visible light because it has a higher band gap and its electron–hole pair recombination is much faster than the reduction, another catalyst must be added in order to make it a visible light-induced photocatalyst; some previously used photocatalyst results have also been shown with the current research in the following Table 4.

Table 4. Comparison with previous results.

Photocatalyst	Rate of Methanol Formation (μmol/g_{cat}·h)	Solvent/Electrolyte	Light Source	Reference
$ZnFe_2O_4/TiO_2$	141.22	Na_2S, Na_2SO_3, KOH in Water	500 W Xenon Lamp	This Study
15% Bi_2S_3/CdS	122.6	NaOH and Na_2S in Water	500 W Xenon Lamp	[23]
CeF_3/TiO_2	80	Water	500 W Xenon Lamp	[14]
Cu_2O/SiC	39	NaOH and Na_2SO_3 in Water	500 W Xenon Lamp	[16]

The above table shows that the current research shows a maximum yield of 141.22 μmol/g_{cat}·h of methanol as compared to other catalysts using the same source of light i.e., a 500-W tungsten Bulb.

Photocatalyst used for the conversion of carbon dioxide into useful fuel with enhanced yield by using visible light could be a most important technique of current era because it can give us Carbon reduction with a fuel. Moreover selective product could be achieved by controlling conduction band position as illustrated by previous research [23,24]. Researchers also suggest that maximum yield still couldn't be achieved due to the reason of formation of other products like formaldehyde, formic acid as well as backward reaction [25].

3. Materials and Method

3.1. Synthesis Procedure

Altered process conditions were used to synthesized the $ZnFe_2O_4/TiO_2$photocatlyst for which initially Zinc nitrate, $Zn(NO_3)_2{\cdot}4H_2O$, and iron nitrate $Fe(NO_3)_3{\cdot}9H_2O$ were dissolved in 2.5 M of HNO_3 and nutrient agar solution, at continuous stirring and heating continuously until a brown–blackish gel was formed. A similar procedure was followed with TiO_2, which was dissolved in 2.5 M of HNO_3 and nutrient agar solution, stirred, and heated continuously until an orange gel was formed. Then, to form the desired band gap, the photocatlyst $ZnFe_2O_4/TiO_2$ was sonicated and calcined at different temperatures for approximately 4.5 h in the presence of N_2 gas. Figure 11 explains the steps involved in the synthesis of the photocatalyst.

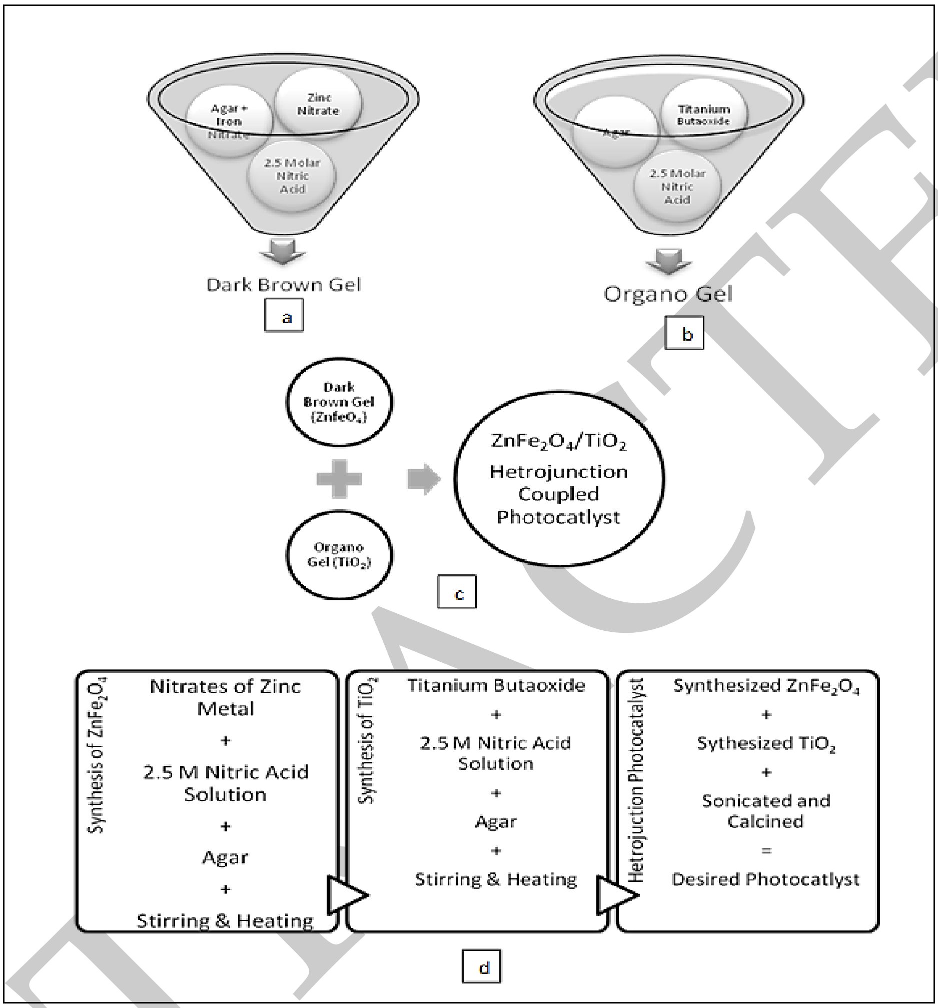

Figure 11. (**a**) Steps involved in synthesis of zinc ferrite, (**b**) steps involved in synthesis of titanium dioxide, (**c**) coupling of zinc ferrite and titanium dioxide, (**d**) detailed steps involved in synthesis of the photocatalyst.

3.2. *Electron and Hole Pair Formation*

The following equations represent concepts of electron and hole pair formation.

$$\text{Photocatalyst} + h\upsilon \rightarrow h^{+} + e^{-} \quad (1)$$

$$h^{+} + e^{-} \rightarrow \text{Heat} \quad (2)$$

$$\text{Eg} \rightarrow \text{Ec} - \text{E}\upsilon \quad (3)$$

where

Eg = band gap energy;
Ec = energy of the conduction band; and
Ev = energy of the valance band.

The photocatalyst when exposed under light irradiation produced the excited electrons and holes, as shown in Equation (1). The electrons start recombining with each other if no absorbed species are present, as shown in Equation (2). This indicates that electron and hole pairs can combine with each other without taking part in oxidation and reduction reactions. As a result, reaction heat is released. If electron and hole pairs have enough energy, they move toward the surface and take part in the reaction. The electron and hole pairs can also be formed on the catalyst surface and produce unproductive heat. Equation (3) represents the band gap calculations as a difference between the valence band and conduction band. The activity of the catalyst depends upon the arrangement of the reaction medium, the absorption capacity of chemicals on the semiconductor's surface, the type of semiconductor and its morphology, and the capacity of the catalyst to absorb UV–Vis light irradiation. Surface improvement and reducing the band gap of a photocatalyst are two major factors.

Methanol production via a CO_2 reduction mechanism through a $ZnFe_2O_4/TiO_2$ photocatalyst is described as shown in Equations (4)–(8). pH has been maintained around 5.9–6.2 such that CO_2 could not only exist as dissolved CO_2 but also in the form of HCO_3^-. The most abundant form of CO_2 at the said pH is dissolved CO_2 and HCO_3^-. The proton balance for this is shown by Equation (4).

$$[H^+] = [OH^-] + [HCO_3^-] + 2\,[CO_3^{2-}] \tag{4}$$

The coefficient 2 in Equation (4) indicates that 2 moles of H^+ are required for the conversion of CO_3^{2-} into HCO_3^- and is considered as a reference level.

The pH of the reaction and during the whole reaction was kept and maintained at around 5.9–6.2, which are acidic values such that all the bicarbonates that can be produced in CO_2 and water mixture can be deserted.

So, it results in another relation as expressed by Equation (5).

$$[H^+]\rightarrow[HCO_3^-] \tag{5}$$

Potassium hydroxide was used to increase the absorbance of CO_2 into water, so the proton balance is shown as per Equation (6).

$$[HCO_3^-] + [H^+]\rightarrow[OH^-] + [CO_3^{2-}] \tag{6}$$

The pH of the solution was very close to a neutral value, so the $[H^+]$ and $[OH^-]$ can be ignored easily.

So, it results in another relation as expressed by Equation (7).

$$[HCO_3^-] = [CO_3^{2-}] \tag{7}$$

The conversion of CO_2 occurs when the reduction reaction on the surface of the synthesized catalyst is done as per Equation (8).

$$CO_2 + 6H^+ + 6e^-\rightarrow CH_3OH + H_2O \tag{8}$$

The reduction potential of CO_2 into methanol falls between the conduction band and valance band of $ZnFe_2O_4/TiO_2$, which means that the coupled semiconductor can reduce CO_2 into methanol. The band gap of $ZnFe_2O_4$ is lower, that is, 1.9 eV; hence, it works under visible light irradiation in comparison with TiO_2, which has a band gap of approximately 3.2 eV.

3.3. Experimental Setup and Operating Conditions

An experimental setup includes a continuous flow reactor followed by a 500 Watt Xenon lamp, which is used as a visible light/radiation source. $NaNO_2$ (2 M) solution was used to cut the UV light. First of all, 0.1 M sodium sulfite, potassium hydroxide, and 0.1 M sodium sulfide were added in 500 mL of distilled water. In the next step, CO_2 fizzed from the solution in the reactor for 1 h to assure that O_2

(dissolved) is approaching toward elimination and the pH of the solution is maintained at 6.2. Moreover, the catalyst should be mixed to the solution, making the concentration of catalyst 1 g/L. Afterwards, the photoreaction started as soon as the 500-watt bulb was switched on. The reactor temperature was maintained at 25 °C with the help of a chiller during the reaction. The CO_2 continuously flowed through the solution during irradiation. Three liquid samples were collected and analyzed in GC-FID for product detection. The photocatalytic reaction was carried out for 6 h. The experimental results of the methanol yield have been confirmed by repeating it three times, and the average yield was taken.

Methanol was analyzed by GC-FID, and a DB-WAX 123-7033 column was used for the detection of methanol. Helium gas was introduced as the shipper gas, and the flow rate was 35 cm/s. The oven temperature was adjusted at 40 °C, and inlet temperature was fixed at 200 °C. The split ratio was 1:50 and the FID temperature was 300 °C. Nitrogen gas was used as the makeup with a flow rate of 30 mL/min at the FID detector. The yield was calculated by using the following equation.

$$Y = (C \times W/V) \quad (9)$$

Y = yield
C = methanol concentration, μmol/L
V = volume, L
W = mass of catalyst, g

4. Conclusions

The primary object of the research was to synthesize a photocatalyst ($ZnFe_2O_4/TiO_2$) as a visible light-induced photocatalyst for the conversion of CO_2into methanol under visible light irradiation. $ZnFe_2O_4$and$ZnFe_2O_4/TiO_2$heterojunction photocatalysts were synthesized and used for the reduction of CO_2into methanol. The most optimized catalyst loading amount was 1g/L to get a maximum yield of methanol. The maximum yield observed was 141.22 $\mu mol/g_{cat}\cdot h$. The prominent feature of this study is to analyze the effect of different parameters on the methanol yield such as the effect of calcination temperature, the intensity of light, the catalyst loading ratio, the effect of different coupling ratios, and the effect of recycling the catalyst. However, as the pH of the reaction solution was maintained at 5.9–6.2; hence, the pH and the most dominant species were 2 and HCO_3^-. The reported yield of methanol obtained by $ZnFe_2O_4/TiO_2$ is quite better because of e^- and H^Ihaving a slow recombination rate due to the formation of the heterojunction. A 7% increase in the yield indicates that the coupling of $ZnFe_2O_4$ with a TiO_2 increases the photocatalytic activity. The coupling of $ZnFe_2O_4/TiO_2$ resulted in a new band gap and made it visible light-responsive. Moreover, the maximum yield has been obtained at a calcination temperature of 900 °C and the coupling ratio is 1:1 *w*/*w*. Hence, after considering all the essential parameters, the results indicate that coupling of $ZnFe_2O_4$ with TiO_2 is effectively enhanced under visible light irradiation. Thus, the following recommendations still need to be considered for future studies.

5. Recommendations

There are some suggestions for the future studies on the synthesis of $ZnFe_2O_4$ and $ZnFe_2O_4/TiO_2$ for the reduction of CO_2 into methanol or some other photocatalytic applications. Despite the fact that $ZnFe^I{}_2O_4$ is a visible light-induced catalyst and forms a heterojunction with TiO_2, which proved itself a very suitable technique for CO_2 reduction, other metal ferrites should also be tested.

Photoreactors of different types should be designed and tested in order to identify the most suitable photoreactor.

Author Contributions: Authors contributed a lot and despite of the busy schedule, gather as when required basis to discuss the conceptualization of the said research. N.M. and M.S. wrote the manuscript, investigate and validate the results. N.M. and U.S. performed data analysis and data curation. S.R.N. supervised, editing and

review the work and in cooperation with N.M. performed project administration. All authors have read and agreed to the published version of the manuscript.

Funding: This research received no external funding.

Conflicts of Interest: The authors declare no conflict of interest.

References

1. Moniz, S.J.A.; Shevlin, S.A.; Martin, D.J.; Guo, Z.-X.; Tang, J. Visible-light driven heterojunction photocatalysts for water splitting–acritical review. *Energy Environ. Sci.* **2015**, *8*, 722–765. [CrossRef]
2. Su, M.; He, C.; Sharma, V.K.; AsiAbou, M.; Xia, D.; Li, X.Z.; Deng, H.; Xiong, Y. Mesoporous zinc ferrite: Synthesis, characterization, and photocatalytic activity with H_2O_2/visible light. *J. Hazard. Mater.* **2012**, *211*, 88–111. [CrossRef] [PubMed]
3. Ola, O.; Maroto-Valer, M.M. Review of material design and reactor engineering on TiO_2 photocatalysis for CO_2 reduction. *J. Photochem. Photobiol. C Photochem. Rev.* **2015**, *24*, 13–49. [CrossRef]
4. Tan, C. CO_2 utilization. *Ind. Mater.* **2013**, *316*, 79–98.
5. AbdelDayem, H.M.; AbdelDayem, S.S.; Hassan, S.A. Selective methanol oxidation to hydrogen over Ag/ZnO catalysts doped with mono-and bi-rare earth oxides. *Ind. Eng. Chem. Res.* **2014**, *53*, 19872–19899. [CrossRef]
6. Heffer, P.; Prud'homme, M. Fertilizer outlook 2013–2017. In Proceedings of the 81st International Fertilizer Industry Association Conference, Chicago, IL, USA, 20–22 May 2013; pp. 7–9.
7. Casbeer, E.; Sharma, V.K.; Li, X. Synthesis and photocatalytic activity of ferrites under visible light: A review. *Sep. Purif. Technol.* **2012**, *87*, 1–17. [CrossRef]
8. Karamian, R.; Ghasemlou, F. Total phenolic content, antioxidant and antibacterial activities of three Verbascum species from Iran. *J. Med. Plants By-Prod.* **2013**, *1*, 42–56.
9. Kawamura, S.; Egami, H.; Sodeoka, M. Amino tri-fluoro methylation of olefins via cyclic amine formation: Mechanistic study and application to synthesis of trifluoro methylated pyrrolidines. *J. Am. Chem. Soc.* **2015**, *137*, 4859–4878. [CrossRef]
10. Matsumoto, Y.; Kim, K.; Bogenhagen, D.F. Proliferating cell nuclear antigen-dependent abasic site repair in Xenopus laevis oocytes: An alternative pathway of base excision DNA repair. *Mol. Cell. Biol.* **1994**, *14*, 6175–6199. [CrossRef]
11. Tahir, M.; Amin, N.S. Advances in visible light responsive titanium oxide based photocatalysts for CO_2 conversion to hydrocarbon fuels. *Energy Convers. Manag.* **2013**, *76*, 192–217. [CrossRef]
12. Uddin, M.N.; Afrin, R.; Uddin, M.J.; Md. Uddin, M.J.; Alam, A.H.M.K.; Rahman, A.A.; Sadik, G. Vanda roxburghii chloroform extract as a potential source of polyphenols with antioxidant and cholinesterase inhibitory activities: Identification of a strong phenolic antioxidant. *BMC Complementary Altern. Med.* **2015**, *15*, 192. [CrossRef] [PubMed]
13. Rekhila, G.; Bessekhouad, Y.; Trari, M. Visible light hydrogen production on the novel ferrite $NiFe_2O_4$. *Int. J. Hydrog. Energy* **2013**, *38*, 6331–6348. [CrossRef]
14. Moualkia, H.; Rekhila, G.; Izerrouken, M.; Mahdjoub, A.; Trari, M. Influence of the film thickness on the photovoltaic properties of chemically deposited CdS thin films: Application to the photodegradation of orange. *Mater. Sci. Semicond. Process.* **2014**, *21*, 181–197. [CrossRef]
15. Li, H.; Lei, Y.; Huang, Y.; Fang, Y.; Xu, Y.; Zhu, X.; Li, X. Photocatalytic reduction of carbon dioxide to methanol by Cu_2O/SiCN an ocrystallite under visible light irradiation. *J. Nat. Gas. Chem.* **2011**, *20*, 142–151.
16. Ghosh, A.; Mangalvedhe, N.; Ratasuk, R.; Mondal, B.; Cudak, M.; Visotsky, E.; Thomas, T.A.; Andrews, J.G.; Xia, P.; Jo, H.S.; et al. Heterogeneous cellular networks: From theory to practice. *IEEE Commun. Mag.* **2012**, *50*, 52–67. [CrossRef]
17. Hao, F.; Lakshman, T.V.; Sarit, M.; Song, H. Providing Cloud-Based Services Using Dynamic Network Virtualization. U.S. Patent No. 9,210,065, 22 June 2015.
18. Kezzim, A.; Nasrallah, N.; Abdi, A.; Trari, M. Visible light induced hydrogen on the novel hetero-system $CuFe_2O_4/TiO_2$. *Energy Convers. Manag.* **2011**, *52*, 2798–2810. [CrossRef]
19. Elias, D.C.; Nair, R.R.; Mohiuddin, T.M.; Morozov, S.V.; Blake, P.; Halsall, M.P.; Ferrari, A.C.; Boukhvalov, D.W.; Katsnelson, M.I.; Geim, A.K.; et al. Control of graphene's properties by reversible hydrogenation: Evidence for graphane. *Science* **2009**, *323*, 605–618. [CrossRef]

20. Kim, M.; Choi, J.-S.; Toops, T.J.; Jeong, E.-S. Coating SiO_2 support with TiO_2 or ZrO_2 and effects on structure and CO oxidation performance of Pt catalysts. *Catalysts* **2013**, *3*, 81–108. [CrossRef]
21. Islam, M.A.; Woon, C.W.; Ethiraj, B.; Cheng, C.K.; Yousuf, A.; Khan, M.M.R. Ultrasound driven biofilm removal for stable power generation in microbial fuel cell. *Energy Fuels* **2016**, *31*, 962–979. [CrossRef]
22. Li, X.; Liu, A.; Chu, D.; Zhang, C.; Du, Y.; Huang, J.; Yang, P. High performance of manganese porphyrin sensitized type $CuFe_2O_4$ photocathode for solar water splitting to produce hydrogen in a tandem photoelectrochemical cell. *Catalysts* **2018**, *8*, 109.
23. Akhter, P.; Farkhondehfal, M.A.; Hernández, S.; Hussain, M.; Fina, A.; Saracco, G.; Khan, A.U.; Russo, N. Environmental issues regarding CO_2 and recent strategies for alternative fuels through photocatalytic reduction with titania-based materials. *J. Environ. Chem. Eng.* **2016**, *4*, 3933–3951. [CrossRef]
24. Lv, M.; Liu, H. Photocatalytic property and structural stability of CuAl-based layered double hydroxides. *J. Solid State Chem.* **2015**, *227*, 229–241. [CrossRef]
25. Xia, S.; Meng, Y.; Zhou, X.; Xue, J.; Pan, G.; Ni, Z. Ti/ZnO–Fe_2O_3 composite: Synthesis, characterization and application as a highly efficient photo-electron catalyst for methanol from CO_2 reduction. *Appl. Catal. B Environ.* **2016**, *187*, 119–136. [CrossRef]